Icarus 233 (2014) 36–47

Contents lists available at ScienceDirect

Icarus

journal homepage: www.elsevier.com/locate/icarus

The formation of supercooled brines, viscous liquids, and low-temperature perchlorate glasses in aqueous solutions relevant to Mars

J.D. Toner [a,*], D.C. Catling [a], B. Light [b]

[a] University of Washington, Department of Earth & Space Sciences, Seattle, WA 98195, USA
[b] Polar Science Center, Applied Physics Laboratory, University of Washington, Seattle, WA 98105, USA

ARTICLE INFO

Article history:
Received 10 July 2013
Revised 4 December 2013
Accepted 19 January 2014
Available online 29 January 2014

Keywords:
Mars
Ices
Astrobiology
Mars, surface

ABSTRACT

Salt solutions on Mars can stabilize liquid water at low temperatures by lowering the freezing point of water. The maximum equilibrium freezing-point depression possible, known as the eutectic temperature, suggests a lower temperature limit for liquid water on Mars; however, salt solutions can supercool below their eutectic before crystallization occurs. To investigate the magnitude of supercooling and its variation with salt composition and concentration, we performed slow cooling and warming experiments on pure salt solutions and saturated soil-solutions of $MgSO_4$, $MgCl_2$, NaCl, $NaClO_4$, $Mg(ClO_4)_2$, and $Ca(ClO_4)_2$. By monitoring solution temperatures, we identified exothermic crystallization events and determined the composition of precipitated phases from the eutectic melting temperature. Our results indicate that supercooling is pervasive. In general, supercooling is greater in more concentrated solutions and with salts of Ca and Mg. Slowly cooled $MgSO_4$, $MgCl_2$, NaCl, and $NaClO_4$ solutions investigated in this study typically supercool 5–15 °C below their eutectic temperature before crystallizing. The addition of soil to these salt solutions has a variable effect on supercooling. Relative to the pure salt solutions, supercooling decreases in $MgSO_4$ soil-solutions, increases in $MgCl_2$ soil-solutions, and is similar in NaCl and $NaClO_4$ soil-solutions. Supercooling in $MgSO_4$, $MgCl_2$, NaCl, and $NaClO_4$ solutions could marginally extend the duration of liquid water during relatively warm daytime temperatures in the martian summer. In contrast, we find that $Mg(ClO_4)_2$ and $Ca(ClO_4)_2$ solutions do not crystallize during slow cooling, but remain in a supercooled, liquid state until forming an amorphous glass near −120 °C. Even if soil is added to the solutions, a glass still forms during cooling. The large supercooling effect in $Mg(ClO_4)_2$ and $Ca(ClO_4)_2$ solutions has the potential to prevent water from freezing over diurnal and possibly annual cycles on Mars. Glasses are also potentially important for astrobiology because of their ability to preserve pristine cellular structures intact compared to solutions that crystallize.

1. Introduction

Liquid water on Mars is important for habitability, weathering of the regolith, and H_2O/CO_2 cycling in the atmosphere; however, pure liquid water is not stable due to the low temperature, relative humidity, and pressure conditions on the surface of Mars (Haberle et al., 2001; Ingersoll, 1970). A way in which water could be stabilized is by the addition of dissolved salts. Salts are common in arid environments, and carbonates (Bandfield et al., 2003; Ehlmann et al., 2008; Morris et al., 2010), sulfates (Kounaves et al., 2010b; Langevin et al., 2005; Murchie et al., 2009), chlorides (Osterloo et al., 2010; Ruesch et al., 2012), and perchlorates (Hecht et al., 2009) have been detected on Mars. Chloride, perchlorate, and some sulfate salts are highly soluble, even at low temperatures, and will lower the activity of water when dissolved at high concentrations. Lower water activities make it possible for liquid water to exist on the surface of Mars due to freezing-point depression (Brass, 1980; Fairén et al., 2009; Kuz'min and Zabalueva, 1998; Marion et al., 2010), deliquescence (Davila et al., 2010; Gough et al., 2011; Zorzano et al., 2009), and lower rates of evaporation (Altheide et al., 2009; Chevrier et al., 2009a; Sears and Chittenden, 2005). On present-day Mars, the presence of liquid water is supported by the distribution of perchlorate in Phoenix soils (Cull et al., 2010), observations of Recurring Slope Lineae (RSL) (Chevrier and Rivera-Valentin, 2012; Martínez and Renno, 2013; McEwen et al., 2011), and observations (albeit controversial) of hygroscopic brine globules on the Phoenix Lander struts (Rennó et al., 2009).

---

* Corresponding author.
E-mail address: toner2@uw.edu (J.D. Toner).

http://dx.doi.org/10.1016/j.icarus.2014.01.018
0019-1035/© 2014 Elsevier Inc. All rights reserved.

Table 1
Salt systems and concentrations selected for this study. Eutectic temperatures were determined in FREZCHEM, except where otherwise noted.

Salt system	Eutectic temperature (°C)	Initial concentrations used (molal)
$MgSO_4$	−3.6	1.65, 2.15, 2.8
$MgCl_2$	−33.0	2.8, 4.8, 5.45, 5.75
$Mg(ClO_4)_2$	−57[a]	3.4, 4.2
NaCl	−21.3	5, 6
$NaClO_4$	−34.1[b]	8.5, 12, 16
$Ca(ClO_4)_2$	−74.4	4, 7

[a] Stillman and Grimm (2011).
[b] Hennings et al. (2013a,b).

The stability of aqueous salt solutions at varying temperatures on Mars has been investigated through equilibrium models (e.g. Chevrier et al., 2009a; Marion et al., 2010). Equilibrium models predict that the lowest temperature a salt solution will remain liquid is the eutectic temperature, at which point a salt solution will solidify to a mixture of ice and salt. Of the common carbonate and sulfate salts of Ca, Mg, Na, and K, eutectic temperatures are relatively high, indicating that these salts will not form low-temperature liquid water on Mars. A notable exception is ferric sulfate ($Fe_2(SO_4)_3$), found in abundance at Gusev crater (Johnson et al., 2007; Lane et al., 2008), which is estimated to have a eutectic temperature of −26.8 °C (Hennings et al., 2013a). Previously, Chevrier and Altheide (2008) had suggested a much lower eutectic for $Fe_2(SO_4)_3$, near −68 °C; however, the phase change they measured was probably the glass transition and not the eutectic (Hennings et al., 2013a). $CaCl_2$ and $Ca(ClO_4)_2$ salts have extremely low eutectic temperatures at −49.4 °C and −74.4 °C respectively. Although it is unlikely that these salts are present on the surface of Mars because Ca^{2+} precipitates strongly with HCO_3^- and SO_4^{2-} (Marion et al., 2009; Toner et al., in preparation), a recent study by Toner and Sletten (2013) in the Dry Valleys of Antarctica found that Ca–Mg–Cl-rich brines can form in the subsurface of frozen soils through cation exchange reactions, and similar processes may occur in martian soils. Furthermore, a recent reanalysis of data from the Wet Chemistry Laboratory (WCL) on the Mars Phoenix Lander suggests that $Ca(ClO_4)_2$ is the dominate perchlorate salt in the soil (Kounaves et al., 2014). Other chloride and perchlorate salts with low eutectic temperatures that have been inferred for martian soils include $MgCl_2$ (−33 °C), $Mg(ClO_4)_2$ (−57 °C), NaCl (−21.3 °C), and $NaClO_4$ (−34.3 °C) (Marion et al., 2010; Toner et al., in preparation).

Eutectic temperatures have generally been interpreted as the lower temperature limits for liquid water on Mars (Brass, 1980; Möhlmann and Thomsen, 2011), but it is well-known that salt solutions can supercool below temperatures where equilibrium models indicate crystallization of salt or ice (Angell and Sare, 1970; Mullin, 2004; Reischel and Vali, 1975). The reason for this supercooling effect is that the nucleation of a crystal from solution requires the energetic formation of a new interface between the crystal surface and the surrounding liquid. The energy requirement for this new interface is supplied by supersaturating the solution until the free energy of crystallization is greater than interfacial surface tension preventing the nucleation of stable crystal nuclei. Once stable crystal nuclei form, the new crystal interfaces serve as a template for further crystallization and crystallization proceeds rapidly towards equilibrium. Supersaturation is often achieved by cooling a solution below its equilibrium freezing point, forming a supercooled solution.

Given the large diurnal temperature fluctuations on the surface of Mars (e.g. Zent et al., 2010), supercooling is likely to occur, and several studies have found evidence for supercooled brines. Stillman and Grimm (2011) found possible evidence for supercooling and eutectic melting of either $NaClO_4$ or $MgCl_2$ brines at the Phoenix lander site based on soil dielectric permittivity and temperature measured by the Thermal and Electrical Conductivity Probe (TECP). No evidence for $Mg(ClO_4)_2$ precipitation was found, indicating that this salt was either not present or is capable of existing in a supercooled state for several hours. As discussed by Stillman and Grimm (2011), $Mg(ClO_4)_2$ brines are particularly prone to supercooling, a property that may have compromised experimentally determined freezing-point depressions in $Mg(ClO_4)_2$ solutions measured by Dobrynina et al. (1980) and Pestova et al. (2005). Gough et al. (2011) investigated metastability under varying relative humidity conditions and found that $NaClO_4$ and $Mg(ClO_4)_2$ solutions readily supersaturate without crystallizing salt. Furthermore, Gough et al. (2011) found that $NaClO_4$ solutions remained liquid down to −50 °C, about 15 °C below the $NaClO_4$ eutectic at −34.1 °C (Hennings et al., 2013b).

To investigate the magnitude of supercooling in aqueous salt solutions and how supercooling is affected by salt composition, concentration, and the presence of soil, we monitored solution temperatures of pure salt solutions and soil-solutions during slow cooling and warming laboratory experiments. By analyzing the temperature profiles from these experiments, we quantified the degree of supercooling that occurs and inferred the composition of salt precipitates.

2. Methods

2.1. Freezing and warming experiments

Solutions were cooled using walk-in freezers (for temperatures down to −30 °C), an ECOSPHERE 307 Environmental Chamber (for temperatures down to −70 °C), and a liquid nitrogen freezing system (for temperatures below −70 °C). Solution temperatures during freezing and warming were continuously monitored at 10 s intervals to an accuracy of ±0.1 °C using LakeShore PT-111 Platinum Resistance Thermometers (PRTs) connected to a CR-10X Campbell Datalogger in a four-wire half-bridge. The PRTs were calibrated at 0 °C in a crushed-ice bath prior to each run.

For the walk-in freezer and environmental chamber experiments, slow cooling rates were achieved by placing salt solutions in a 30 × 30 × 30 cm polystyrene insulating block with a central cavity (approximately 200 cm^3) for holding the solutions. During a typical experiment, 20 g of salt solution was poured into a plastic bag. The plastic bag holding the solution was then folded over and taped, creating a pocket for the PRT. This ensured that the PRT was not exposed to the corrosive salt solution and that the PRT was surrounded by solution on all sides. The bagged solutions were then placed within the polystyrene insulation, which slowed the rate of cooling and minimized heat absorption by surrounding materials. After cooling to the freezer temperature, the solutions were allowed to warm slowly by placing the solutions, still surrounded by polystyrene insulation, into ambient air at room temperature. To achieve temperatures below −70 °C, we constructed a passive liquid nitrogen freezing system (Fig. 1). This system is comprised of a steel vessel with a smaller aluminum vessel placed inside. A cylinder of polystyrene foam, with a central cavity for holding solutions, was placed in the interior aluminum vessel. Liquid nitrogen was poured into the cavity separating the two vessels, which cooled the interior of the aluminum vessel. The outer steel vessel was placed in a large plastic tub filled with spray-on insulation. Solutions cooled in the liquid nitrogen freezing system were allowed to passively warm to room temperature once the liquid nitrogen had completely evaporated.

Time-dependent temperature profiles indicate when solid phases either crystallize from solution or dissolve into solution. As salt solutions are cooled from room temperature, they become supercooled with respect to either ice or salt below the equilibrium

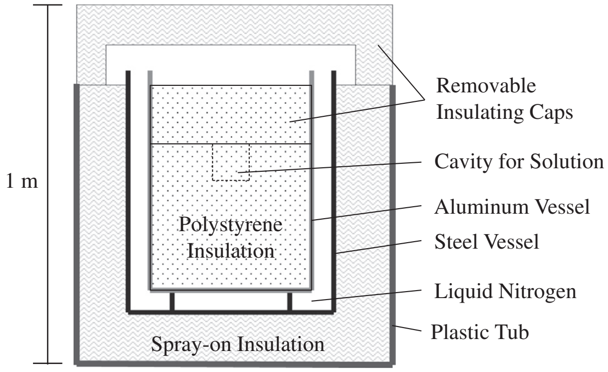

Fig. 1. A schematic of the liquid nitrogen freezing system used to cool solutions below −70 °C.

freezing point. Once supercooling has reached the point where either ice or salt first nucleates from solution, the precipitation reaction occurs rapidly because the solid phase acts as a template for further crystallization. Because precipitation reactions are exothermic, crystallization is indicated by a sudden spike in the temperature profile. Upon warming, a mixture of salt and ice melts endothermically at the equilibrium melting temperature, which causes the temperature profile to become constant with time. In these experiments, we infer the composition of solid phases by considering the temperature plateau upon warming and the number of possible solid phases for each salt system. These inferences are made reasonable by the characteristic nature of the equilibrium melting temperature and the limited number of crystalline phases in binary salt systems (ice + anhydrous/hydrous salts). Furthermore, we differentiate ice precipitation events from salt precipitation events by considering the relative size of temperature spikes; in general, enthalpies of crystallization for salts are much larger than for ice.

2.2. Selected samples

The analysis of water soluble salts by the WCL experiment on the Phoenix lander indicated that the soil is rich in Mg^{2+}, Na^+, ClO_4^-, and SO_4^{2-} (Hecht et al., 2009; Kounaves et al., 2010a,b; Toner et al., in preparation). Based on the observed predominance of Mg^{2+} and Na^+ ions and the inferred composition of salt phases in Phoenix soils (Toner et al., in preparation), we chose to study supercooling in six salt systems: $MgSO_4$, $MgCl_2$, $Mg(ClO_4)_2$, NaCl, $NaClO_4$, and $Ca(ClO_4)_2$ (see Table 1). We include $Ca(ClO_4)_2$ solutions in our investigation for comparison with $Mg(ClO_4)_2$ solutions, and because $Ca(ClO_4)_2$ has been suggested at the Phoenix site by Kounaves et al. (2014) based on transient signals in the WCL data.

All salt solutions were prepared from reagent grade chemicals and deionized water. The concentration of the solution determines which solids will precipitate and the temperature at which equilibrium precipitation first occurs. For example, the equilibrium phase diagram of $MgSO_4$ indicates that a dilute solution will precipitate ice near 0 °C, while a solution with a eutectic concentration of 1.72 m will precipitate both ice and $MgSO_4{\cdot}11H_2O$ at the −3.6 °C eutectic. Higher concentration solutions will precipitate salt ($MgSO_4{\cdot}7H_2O$, $MgSO_4{\cdot}11H_2O$, etc.) before ice. We base our selection of solution concentrations for the freezing/warming experiments on the concentrations at which major phase changes occur in the phase diagram, such as the eutectic temperature and transitions between salt hydrates. All concentrations were chosen to be slightly lower than these major phase changes. In addition, solutions near saturation at room temperature were also cooled.

On Mars, any concentrated salt solutions that exist will likely be in contact with soil. Hence, in addition to investigating pure salt solutions, we also performed cooling and warming experiments on mixtures of soil and salt solution. The experimental procedure is the same as for the pure salt solutions, except that 20 g of soil was added to 20 g of salt solution. We used JSC Mars-1, martian regolith simulant for these experiments (Allen et al., 1998).

3. Results

The results of the cooling/warming experiments are plotted next to phase diagrams created using FREZCHEM (Marion and Kargel, 2008). Any metastable pathways that occur during cooling are indicated by dashed lines in the phase diagrams. These are created by preventing a phase, such as ice, from precipitating in FREZCHEM. In general, the temperature profiles upon cooling are characterized by three main phases: (1) initial rapid cooling, (2) a sequence of one or more spikes in temperature followed by slower cooling rates or a plateau in temperature, and (3) a final rapid temperature decrease. Upon warming, the temperature increases rapidly, followed by a plateau that lasts for several hours, before again increasing rapidly. This sequence of events is similar for all of the salt solutions studied here, except for $Mg(ClO_4)_2$ and $Ca(ClO_4)_2$ solutions, which are discussed later.

3.1. $MgSO_4$ and $MgCl_2$ solutions

3.1.1. $MgSO_4$

As solutions of $MgSO_4$ cool, no precipitation events occur until the temperature drops 4–6 °C below the −3.6 °C eutectic (Fig. 2A and B). After this, two temperature spikes in the 1.65 and 2.15 m $MgSO_4$ solutions indicate two precipitation events, which increase the temperature by about 5 °C and 15 °C respectively. In contrast, only one precipitation event occurs in the 2.8 m $MgSO_4$ solution, increasing the temperature by 2.5 °C. After each precipitation event, the rate of cooling either slows dramatically or plateaus. These lower rates of cooling indicate that heat is being released as ice or salt continuously crystallizes, which slows the cooling of the salt solution. In the 1.65 and 2.15 m $MgSO_4$ solutions, the temperature increase following the second precipitation event abruptly plateaus at the $MgSO_4$ eutectic (−3.6 °C). We infer that the solution at this plateau has a eutectic composition, and that the temperature is stable because heat from exothermic crystallization balances endothermic melting of eutectic solids and thermal diffusion from the system. Finally, once the salt solution has completely solidified, heat is no longer released by crystallization and the ice–salt mixture cools rapidly. The temperature just prior to the last precipitation event is the lowest temperature at which liquid solution remains. In the 1.65 and 2.15 m $MgSO_4$ solutions, the solution remains in a supercooled, liquid state for about 12 h and cools to a maximum of 15.4–15.8 °C below the eutectic temperature before finally solidifying. The 2.8 m $MgSO_4$ solution is much less metastable and cools only 4.2 °C below the eutectic before solidifying.

Upon warming, the $MgSO_4$ solutions melt, which is indicated by a long period of constant temperature due to endothermic melting of the ice–salt mixture. The temperature of this plateau can be used to infer the composition of the precipitated salts. For the 1.65 and 2.15 m $MgSO_4$ solutions, the temperature plateau occurs at −3.6 °C, which is the eutectic temperature of a mixture of ice and meridianiite ($MgSO_4{\cdot}11H_2O$). This indicates that the two precipitation events during cooling were due to ice, followed by $MgSO_4{\cdot}11H_2O$. The melting temperature of the 2.8 m $MgSO_4$ solution is −4.8 °C, which is near the metastable eutectic of −5 °C for a mixture of ice and epsomite ($MgSO_4{\cdot}7H_2O$) (Hogenboom et al., 1995). Because only one precipitation event occurred during

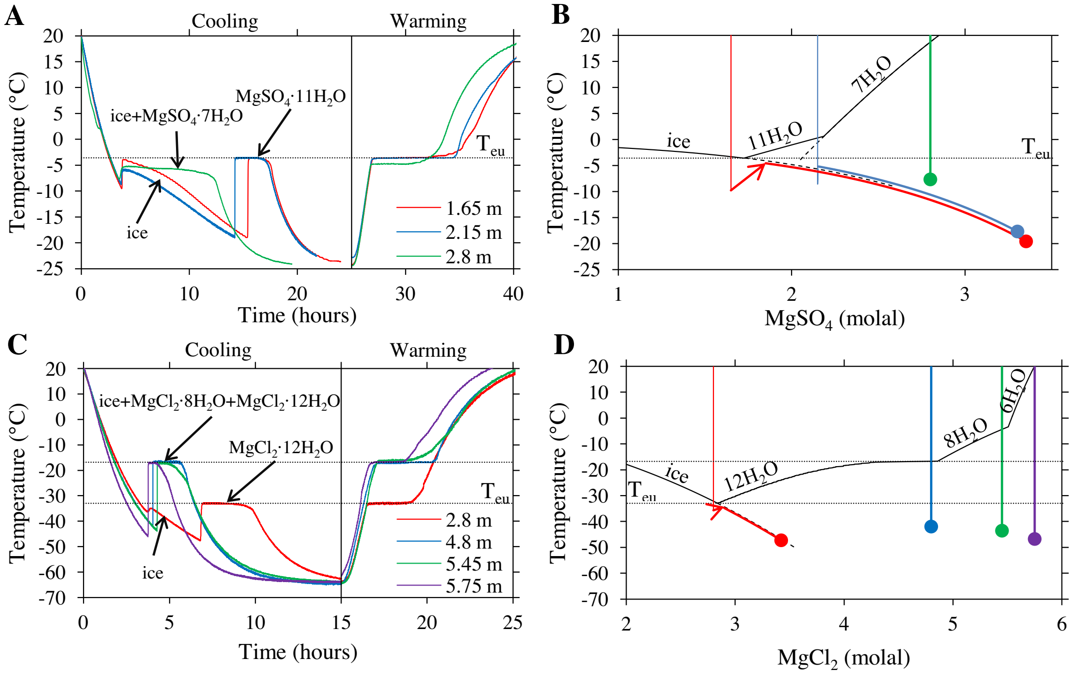

Fig. 2. (A) The temperature of initially 1.65 (red line), 2.15 (blue line), and 2.8 m (green line) $MgSO_4$ solutions during cooling and warming experiments, showing inferred crystallization events. (B) The freezing pathway during cooling of solutions inferred from the sequence of salt precipitation and the degree of supercooling indicated in (A). The dashed lines indicate pathways followed by solutions in equilibrium with one phase, such as ice, but metastable with respect to another, such as salt. Large dots indicate the point just prior to the last precipitation event, which is the lowest temperature at which liquid solution remains; thus, following the metastable lines until the final phase is precipitated. (C) An analogous plot to (A) for initially 2.8 (red line), 4.8 (blue line), 5.45 (green line), and 5.75 m (purple line) $MgCl_2$ solutions, showing inferred crystallization events and the two $MgCl_2$ eutectics at −33 °C and −16.8 °C. (D) Analogous to (B) for the $MgCl_2$ solutions. (For interpretation of the references to colors in this figure legend, the reader is referred to the web version of this paper.)

cooling in the 2.8 m $MgSO_4$ solution, both ice and $MgSO_4·7H_2O$ must have precipitated simultaneously.

3.1.2. $MgCl_2$

The results of the cooling and warming experiments for $MgCl_2$ are similar to the $MgSO_4$ experiments (Fig. 2C and D). The 2.8 m $MgCl_2$ solution is characterized by two precipitation events during cooling; the first event increases the temperature by 1.2 °C, while the second is much more exothermic and increases the temperature by 13.5 °C. In contrast, the 4.8, 5.45, and 5.75 m $MgCl_2$ solutions all have a single, highly exothermic precipitation event during cooling, causing the temperature to spike by 25–30 °C. During warming, the temperature in the 2.8 m $MgCl_2$ solution plateaus at the −33 °C eutectic of ice–$MgCl_2·12H_2O$. In the 4.8, 5.45, and 5.75 m $MgCl_2$ solutions, temperatures plateau at the −16.8 °C peritectic of the $MgCl_2$ system for ice–$MgCl_2·8H_2O$–$MgCl_2·12H_2O$ (Spencer et al., 1990). We infer that in the 2.8 m $MgCl_2$ solution, ice crystallizes first, followed by $MgCl_2·12H_2O$. In contrast, ice, $MgCl_2·8H_2O$, and $MgCl_2·12H_2O$ crystallize simultaneously in the 4.8, 5.45, and 5.75 m $MgCl_2$ solutions.

The $MgCl_2$ solutions supercool 9–14 °C below the −33 °C eutectic before crystallizing salt, which is generally less than supercooling in the $MgSO_4$ solutions. However, compared to the −16.8 °C metastable eutectic, the 4.8, 5.45, and 5.75 m $MgCl_2$ solutions supercool by 25–30 °C. When salt finally crystallizes during cooling, the greater degree of supercooling in the 4.8, 5.45, and 5.75 m $MgCl_2$ solutions relative to the peritectic causes temperatures to increase much more rapidly (50 °C min^{-1}) than in the 2.8 m $MgCl_2$ solution (4 °C min^{-1}).

3.2. NaCl and $NaClO_4$ solutions

The 5 and 6 m NaCl solutions crystallized into ice and hydrohalite ($NaCl·2H_2O$), as indicated by the plateau in temperature at the −21.3 °C NaCl eutectic upon warming (Fig. 3A and B). In the 5 m NaCl solution both ice and $NaCl·2H_2O$ appear to crystallize simultaneously, whereas in the 6 m NaCl solution ice crystallizes first, followed shortly thereafter by $NaCl·2H_2O$. We infer that ice crystallized first because the first temperature spike is much smaller than the second temperature spike and the first precipitation event occurred within the stability region for ice. NaCl solutions supercool between 6.6 and 8.3 °C below the eutectic before forming a eutectic mixture.

The 8.5, 12, and 16 m $NaClO_4$ solutions all crystallize ice and $NaClO_4·2H_2O$, as indicated by the plateau in temperature at the $NaClO_4$ eutectic (−34.3 °C) upon warming (Fig. 3C and D). In the 8.5 m $NaClO_4$ solution, ice crystallization occurs first and $NaClO_4·2H_2O$ crystallization occurs several hours afterward. In contrast, the first precipitation event in the 12 and 16 m $NaClO_4$ solutions occurs far above the temperature where ice should crystallize, indicating that these solutions first crystallize $NaClO_4·2H_2O$ and then ice. $NaClO_4$ solutions supercool between 5.4 and 11.5 °C before forming a eutectic mixture, with supercooling in the 8.5 m $NaClO_4$ solution being the greatest.

3.3. $Mg(ClO_4)_2$ and $Ca(ClO_4)_2$ solutions

The results of cooling $Mg(ClO_4)_2$ and $Ca(ClO_4)_2$ solutions differ from previous results for salts of Mg and Na (Fig. 4). During cooling and warming of the 3.4 and 4.2 m $Mg(ClO_4)_2$ solutions (using 20 g of solution), no spikes in temperature occur, despite cooling down to −170 °C. This suggests that crystallization did not occur. To determine if the solution would crystallize under a slower cooling rate, we reduced the rate of cooling by using 50 g of solution instead of 20 g. During these slower cooling experiments, again no temperatures spikes were measured; however, during warming, an abrupt temperature increase occurs in the 4.2 m $Mg(ClO_4)_2$

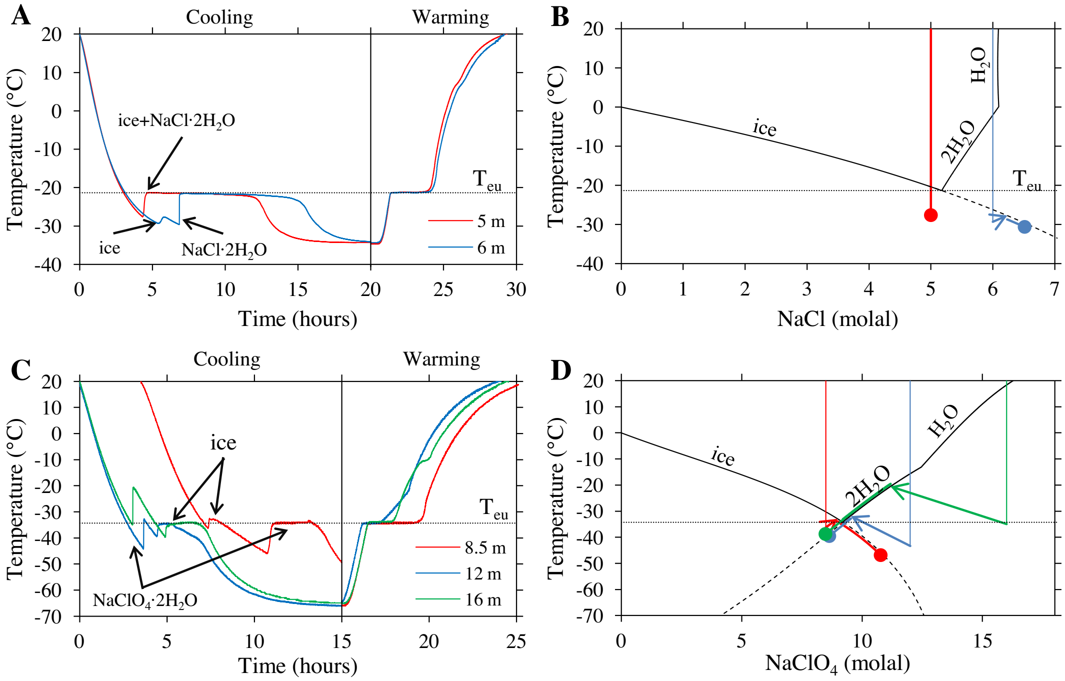

Fig. 3. (A) The temperature of initially 5 (red line) and 6 m (blue line) NaCl solutions during cooling and warming experiments, showing inferred crystallization events. (B) The freezing pathway during cooling of solutions inferred from the sequence of salt precipitation and the degree of supercooling indicated in (A). Large dots indicate the point just prior to the last solid phase precipitation event, which is the lowest temperature at which liquid solution remains. (C) An analogous plot to (A) for initially 8.5 (red line), 12 (blue line), and 16 m (green line) $NaClO_4$ solutions (the 8.5 m profile is staggered for clarity), showing inferred crystallization events. (D) Analogous to (B) for the $NaClO_4$ solutions. (For interpretation of the references to colors in this figure legend, the reader is referred to the web version of this paper.)

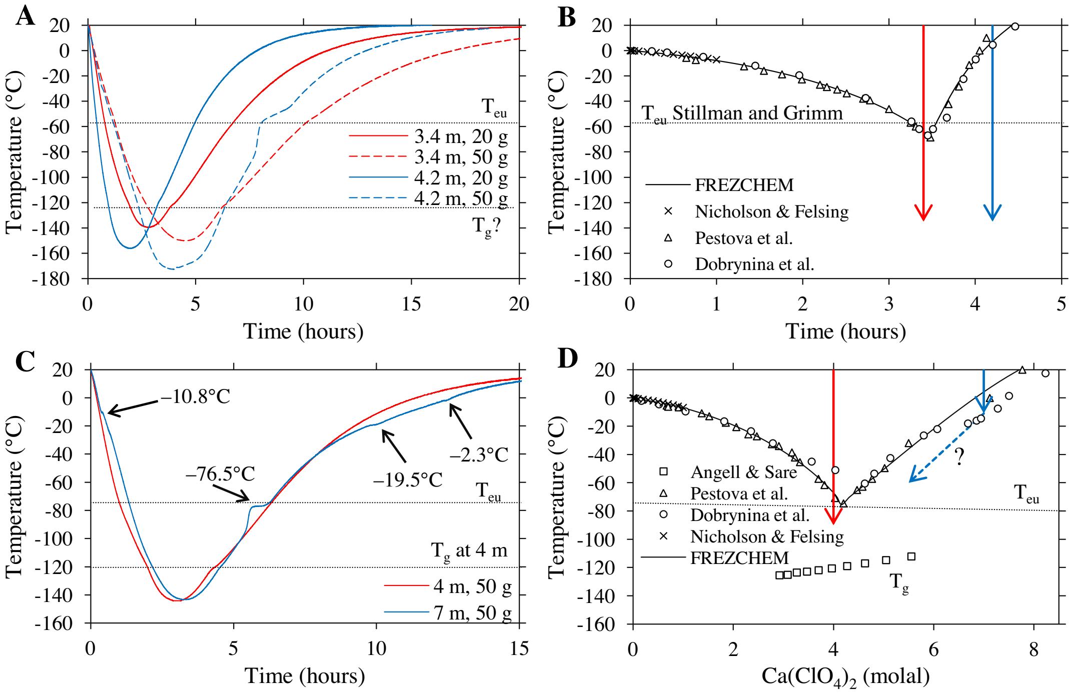

Fig. 4. (A) The temperature of $Mg(ClO_4)_2$ solutions of 3.4 and 4.2 m initial concentration during cooling and warming experiments. Experiments were run with 20 g of solution, as in previous experiments with other salts, and with 50 g of solution to reduce cooling rates. (B) The phase diagram for $Mg(ClO_4)_2$ solutions using FREZCHEM (line) with experimental freezing-point depression and solubilities from Nicholson and Felsing (1950), Pestova et al. (2005), and Dobrynina et al. (1980) (symbols). Arrows show the solution concentrations used and their evolution with cooling. (C) An analogous plot to A for the $Ca(ClO_4)_2$ solutions of 4 and 7 m initial concentration, in which 50 g of solution was used, showing inferred crystallization events and two melting events. (D) Analogous to (B) for $Ca(ClO_4)_2$ solutions. The dashed arrow indicates the probable direction the solution evolves after the salt precipitation event at −10.8 °C, which is uncertain due to uncertainties in the $Ca(ClO_4)_2$ phase diagram. Experimental freezing-point depressions are from Nicholson and Felsing (1950), Pestova et al. (2005), and Dobrynina et al. (1984). Glass transition temperatures (T_g) for $Ca(ClO_4)_2$ solutions are from Angell and Sare (1970).

solution starting near −80 °C. This temperature increase terminates near the −57 °C eutectic for $Mg(ClO_4)_2$ measured by Stillman and Grimm (2011). Above −57 °C, the rate of cooling slows, suggesting that the previously crystallized salt phase began melting above the eutectic.

No crystallization events occur in the 4 m $Ca(ClO_4)_2$ solution; in contrast, there are four distinct precipitation/dissolution events in the 7 m $Ca(ClO_4)_2$ solution. During cooling of the 7 m $Ca(ClO_4)_2$ solution, a very small spike in temperature occurs at −10.8 °C, indicating crystallization. Evidently, the solution did not completely solidify at this point because a large precipitation event occurs during warming starting at about −93 °C and plateauing at −76.5 °C. After this, two more small plateaus in temperature occur at −19.5 °C and −2.3 °C, indicating dissolution events. None of these temperature excursions correlate well with phase changes indicated by $Ca(ClO_4)_2$ phase diagrams, except that the plateau at −76.5 °C is near the −74.6 °C eutectic. We note that there is some disagreement on the $Ca(ClO_4)_2$ phase diagram between Dobrynina et al. (1984) and Pestova et al. (2005). Pestova et al. (2005) measured the $Ca(ClO_4)_2$ eutectic at −74.6 °C, but Dobrynina et al. (1984) measured the $Ca(ClO_4)_2$ eutectic at −60.5 °C and indicate that −75.5 °C is a metastable eutectic. Furthermore, Dobrynina et al. (1984) suggest that $Ca(ClO_4)_2 \cdot 8H_2O$, $Ca(ClO_4)_2 \cdot 4H_2O$, and anhydrous $Ca(ClO_4)_2$ can occur down to −115 °C in both stable and metastable states, whereas Pestova et al. (2005) indicate that only $Ca(ClO_4)_2 \cdot 8H_2O$ forms. Clearly, the $Ca(ClO_4)_2$ phase diagram needs to be revisited.

The general absence of temperature plateaus or spikes in the $Mg(ClO_4)_2$ and $Ca(ClO_4)_2$ cooling experiments suggests that these salt solutions remained liquid at extremely low temperatures. To further investigate these solutions, we slowly cooled some of them down to −150 °C and then removed the samples from the liquid nitrogen freezing system and observed the samples as they warmed in ambient air. Initially, the samples appeared clear and translucent, but were solid, not liquid; this is distinct from the white, opaque appearance of samples that crystallize (Fig. 5). Upon warming to near −120 °C, the samples softened, becoming gel-like in consistency and remaining translucent. Further warming caused the samples to gradually transition to a liquid. These observations and the absence of crystallization events in the $Mg(ClO_4)_2$ and $Ca(ClO_4)_2$ solutions are consistent with vitrification i.e. the transition from a liquid to an amorphous glass during cooling. Vitrification has been studied extensively and is common when electrolyte solutions are cooled rapidly (Angell, 2002; Ediger et al., 1996; Franks, 1993; MacFarlane, 1987), but is rarer during slow cooling. What is remarkable about the $Mg(ClO_4)_2$ and $Ca(ClO_4)_2$ solutions studied here is that these solutions transition to glass in spite of slow cooling rates of <1 °C min^{-1}.

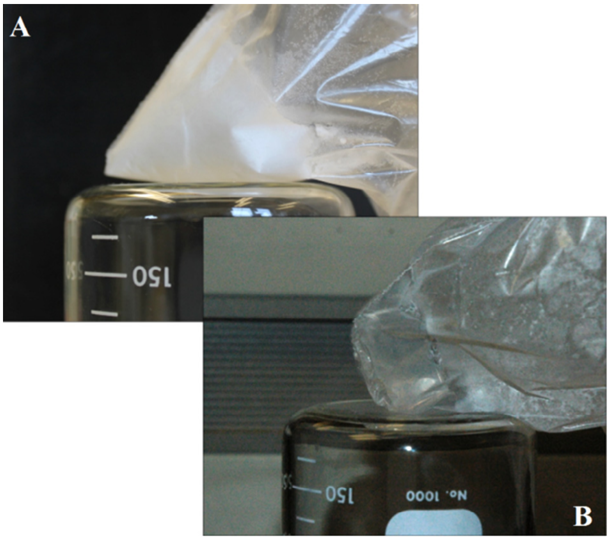

Fig. 5. (A) A solution of 1.65 $MgSO_4$ cooled to a eutectic solid. The solid appears as a white, opaque mass. (B) A clear, vitrified solution of 4 m $Ca(ClO_4)_2$. The solution is turned on its side to show that it does not flow.

Vitrification occurs when the viscosity of a cooled solution increases to $\sim 10^{12}$ Pa s, at which point any crystallization or dissolution reactions become kinetically inhibited and the liquid structure becomes ‘frozen’ in-place. The temperature at which a liquid becomes a glass is known as the glass transition temperature (T_g) and is measured experimentally by identifying a sudden decrease in heat capacity that occurs as temperatures decrease below T_g (Angell and Sare, 1970; Angell and Tucker, 1980), although there are a number of other thermodynamic properties that also change at the glass transition (Angell and Sichina, 1976). In Fig. 4, the occurrence of a glass transition for both $Mg(ClO_4)_2$ and $Ca(ClO_4)_2$ solutions is confirmed by a slight change in the cooling/warming rate near −120 °C. This change in the cooling rate is caused by the sudden decrease in heat capacity below T_g.

T_g has been measured in varying concentration $Ca(ClO_4)_2$ solutions (Angell and Sare, 1970), and for a 4 m $Ca(ClO_4)_2$ solution, T_g is −120 °C (values from Angell and Sare (1970) are shown in Fig. 4D). This correlates well with the temperature at which the rate of cooling and warming changed in our 4 m $Ca(ClO_4)_2$ solution. By extrapolating the relationship between T_g and molality in Angell and Sare (1970) linearly, we infer that the 7 m $Ca(ClO_4)_2$ solution should vitrify at −105 °C; however, the change in cooling rate occurs at about −120 °C instead. This lower than expected value for T_g is consistent with the precipitation of salt at higher temperatures, which would have lowered the concentration of the initially 7 m $Ca(ClO_4)_2$ solution. It is interesting that vitrification still occurs in the 7 m $Ca(ClO_4)_2$ solution, even though a solid phase (salt in this case) crystallized at higher temperatures, evidently forming a mixed glassy-crystalline solid. Alternatively, MacFarlane (1987) notes that it is possible for ice to crystallize from solution, continuously concentrating the remaining solution, until the remaining liquid solution transitions to glass, forming an ice–glass mixture. Hence, it is possible to form either a pure glass, or a mixture of glass and crystalline solid. With respect to the $Mg(ClO_4)_2$ solutions, there are no literature values for T_g, but our data suggests that T_g occurs at −123 °C, similar to the $Ca(ClO_4)_2$ solutions.

In the cases where crystallization does occur upon warming, in the 4.2 m $Mg(ClO_4)_2$ solution and the 7 m $Ca(ClO_4)_2$ solution, crystallization is initiated only when the solution is 30–40 °C above T_g. This is curious because the high degree of supersaturation just above T_g should provide a strong driving force for crystal nucleation. In investigating supercooled aqueous solutions of citric acid, Mullin and Leci (1969) found that below a critical supercooling temperature, the rate of crystal nucleation decreased due to the increasing viscosity of the solution with decreasing temperature. This suggests that there is a temperature range above T_g where highly viscous solutions will remain liquid due to the slow kinetics of crystallization in this region. The upper temperature limit of this viscous state is known as the devitrification temperature (T_d) (MacFarlane, 1986). T_d is measured experimentally by warming a glass slowly and recording the temperature at which crystallization first occurs.

3.4. Saturated soil-solutions

The slow cooling and warming experiments discussed above were done with pure salt solutions; however, on Mars, any salt solutions that exist will be in contact with soil or rock surfaces. In the absence of standing bodies of water, the maximum brine content in soils will be at saturation. Initially, we expected that addition of soil to salt solutions would greatly lower the amount of supercooling because mineral surfaces can act as catalysts for crystal nucleation, an effect known as heterogeneous nucleation (Mullin, 2004). However, contrary to our expectations, the addition of soil to the salt solutions did not strongly reduce the magnitude of supercooling, and for $MgCl_2$ solutions the supercooling was greater (Fig. 6). Only in the 1.65 m $MgSO_4$ soil-solution was supercooling reduced relative to the pure salt solution; the 1.65 m $MgSO_4$ soil-solutions supercooled 6.6 °C below the eutectic, whereas the pure salt solution supercooled 15.5 °C below the eutectic. In the NaCl and $NaClO_4$ soil-solutions, the degree of supercooling below the eutectic was similar to the pure salt solutions within ±1 °C, indicating that the addition of soil has little effect on supercooling. The 2.8 m $MgCl_2$ soil-solution supercooled 17 °C below the −33 °C eutectic, which is greater than the 13.8 °C supercooling measured in the pure salt solution. In contrast to the $MgSO_4$, $MgCl_2$, NaCl, and $NaClO_4$ soil-solutions, $Mg(ClO_4)_2$ and $Ca(ClO_4)_2$ soil-solutions did not crystallize during cooling, but transitioned to a glass. During warming, the 3.4 m $Mg(ClO_4)_2$ soil-solution does crystallize, unlike in the pure 3.4 $Mg(ClO_4)_2$ solution. This crystallization event is characterized by a sudden spike in warming starting at −90 °C, followed by a several-hours-long plateau near the −57 °C eutectic (Stillman and Grimm, 2011). Remarkably, the 4 m $Ca(ClO_4)_2$ soil-solution does not crystallize during either warming or cooling.

4. Discussion

4.1. Supercooling in salty solutions

The results of this study, summarized in Table 2, indicate that the degree of supercooling is highly variable, and depends on the salt composition, concentration, the phase (ice or salt) that is precipitated, and the presence of soil. There are several different ways in which the degree of supercooling can be quantified: (1) the amount of supercooling below the eutectic temperature (ΔT_{eu}) or (2) the temperature difference between when ice or salt precipitated (T_i and T_s respectively) and when ice or salt should have precipitated according to equilibrium models, such as FREZCHEM (the difference being ΔT_i and ΔT_s respectively). ΔT_{eu} ranges between 0.6 and 15.5 °C and does not show any consistent trends with salt composition or concentration. In the $MgSO_4$ and $NaClO_4$ solutions, ΔT_{eu} decreases with concentration, while in the $MgCl_2$ and NaCl solutions, ΔT_{eu} increases with concentration. Both ΔT_i and ΔT_s are strongly dependent on concentration. ΔT_i ranges from 3.3 to 13.8 °C and generally increases with concentration, except for $MgSO_4$ solutions, where it decreases. ΔT_s ranges from 6.3 to

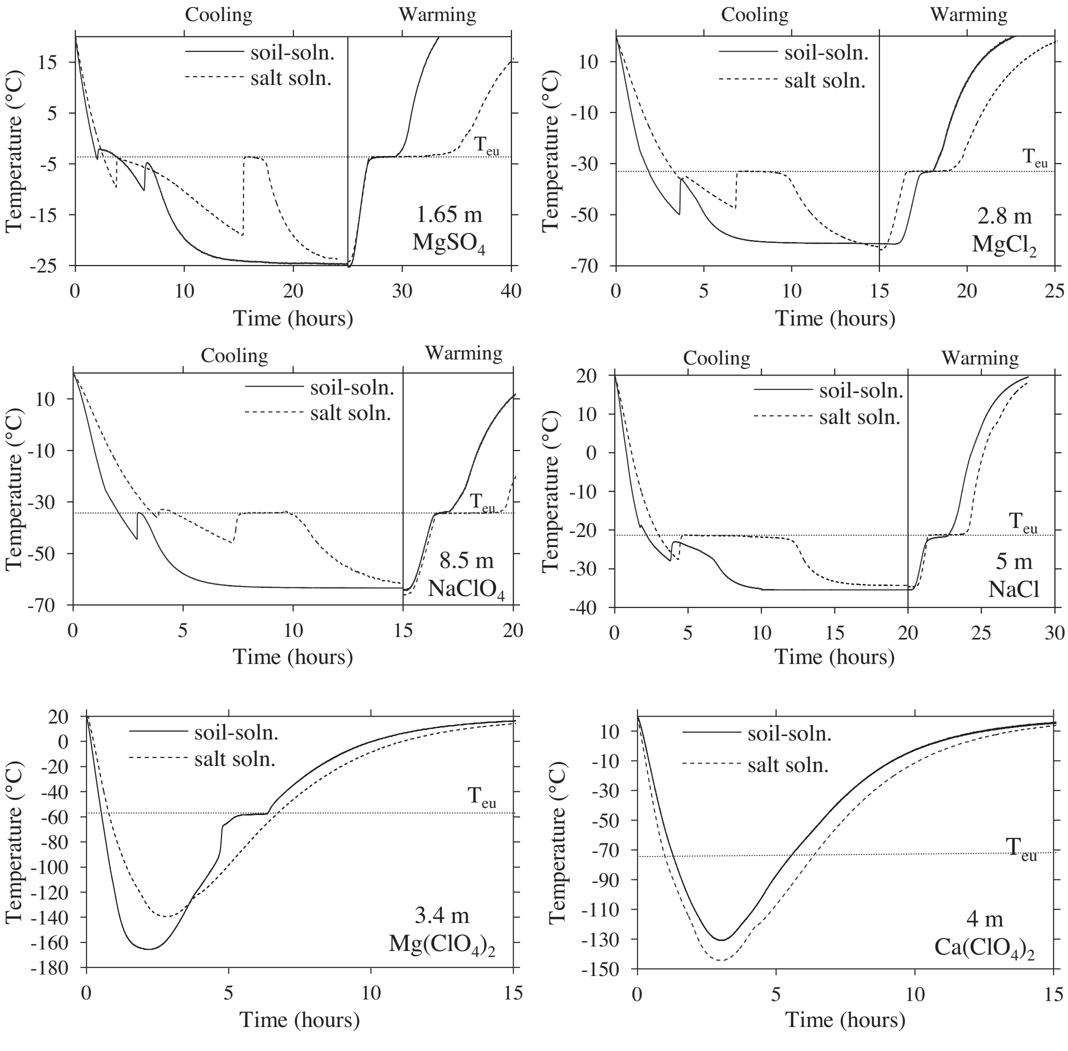

Fig. 6. Supercooling measured during cooling and warming experiments on saturated soil-solutions of $MgSO_4$, $MgCl_2$, $NaClO_4$, NaCl, $Mg(ClO_4)_2$, and $Ca(ClO_4)_2$, using JSC Mars-1 martian soil simulant as the soil (solid lines). The results from pure salt solutions are also shown as dashed lines for comparison.

Table 2
A summary of supercooling results for various concentrations from the non-glass-forming solutions investigated in this study. The eutectic temperature for each salt system is given with the concentration at the eutectic in parentheses. ΔT_{eu} is the amount of supercooling below the eutectic. T_i and T_s are the crystallization temperatures of ice and salt. ΔT_i and ΔT_s are the differences between T_i and T_s and the predictions from the FREZCHEM model.

Salt system	Conc. (m)	Eutectic (°C)	ΔT_{eu} (°C)	T_i (°C)	ΔT_i (°C)	T_s (°C)	ΔT_s (°C)
$MgSO_4$	1.65	−3.6 (1.72 m)	15.5	−9.8	6.4	−19.1	15.5
	2.15		15.1	−8.5	4.9	−18.7	18.9
	2.8		4.1	−7.7	4.1	−7.7	26.4
$MgCl_2$	2.8	−33 (2.84 m)	13.8	−35.5	3.3	−46.8	13.8
	4.8		9.0	−42	9.0	−42.0	25.2
	5.45		10.6	−43.6	10.6	−43.6	39.2
	5.75		13.8	−46.8	13.8	−46.8	67.0
NaCl	5	−21.3 (5.17 m)	6.3	−27.6	7.2	−27.6	6.3
	6		8.4	−29.3	8.0	−29.7	27.5
$NaClO_4$	8.5	−34.3 (9.2 m)	11.5	−36	5.7	−45.8	11.5
	12		9.0	−38.3	4.0	−43.3	27.5
	16		0.6	−39.7	5.4	−34.9	53.1

67 °C and always increases with concentration. ΔT_s is typically much greater than ΔT_i, indicating that salt crystallization is much more prone to metastability than ice crystallization. With respect to solution composition, both ΔT_i and ΔT_s are greater in the Mg solutions than in the Na solutions at similar concentrations. In the $Mg(ClO_4)_2$ and $Ca(ClO_4)_2$ solutions, ΔT_{eu}, ΔT_i, and ΔT_s could not be evaluated because salt precipitation did not occur at any concentration during cooling because glassy and viscous liquid states formed.

There are a number of other variables besides composition and concentration that can influence the degree of supercooling that were not investigated in this study, including: cooling rate, agitation, pressure, and the presence of ionic impurities (Mullin, 2004). Faster cooling typically results in greater supercooling because the timescale for crystallization is reduced, whereas slower cooling results in less supercooling. The relatively slow cooling rates in this study were chosen to mimic temperature changes that might occur over diurnal cycles on Mars. Most of the experiments had maximum cooling and warming rates of ~0.2 °C min^{-1}. The liquid nitrogen system cooled 50 g samples at a rate of ~1 °C min^{-1}, and warmed samples at a rate of ~0.2 °C min^{-1}. Air temperatures measured by the Phoenix Lander indicate that the rate of temperature change is seldom greater than 0.2 °C min^{-1}, which is similar to maximum rates of near-surface soil temperature change measured by the Thermal and Electrical Conductivity Probe (TECP) on the Phoenix Lander. Hence, near-surface rates of temperature change are consistent with the rates used in this study; however, in the subsurface, temperature fluctuations will be damped, causing rates of temperature change to decrease, particularly if subsurface ice is present (Zent et al., 2010). Agitation will increase the kinetic energy in the solution, which will decrease supercooling; however, agitation is not likely to be important on Mars, except possibly at the surface where solutions could be agitated by wind. Ionic impurities are a factor that could potentially greatly increase supercooling. This is because the presence of foreign ions can interfere with crystal growth. For example, it is well known that the growth or nucleation of calcite is kinetically inhibited in solutions containing Mg^{2+}, leading to solutions supersaturated with respect to calcite, such as occurs in seawater (Berner, 1975). We did not study the effects of ionic impurities because we experimented on pure salt solutions, but given that soil solutions on Mars will contain a variety of ions (Kounaves et al., 2010a), this effect is likely important and warrants further study.

Foreign surfaces, such as soil particles, typically decrease supercooling due to heterogeneous nucleation; however, in our experiments freezing salt solutions mixed with JSC Mars-1 soil, a consistent decrease in supercooling was not observed. Furthermore, $Mg(ClO_4)_2$ and $Ca(ClO_4)_2$ solutions still reached the glass transition during cooling. We speculate that the supercooling measured in soil-solution mixtures, despite the nucleating tendency of foreign surfaces, may be due to colloids in the soil suspension. Concentrated colloid suspensions facilitate supercooling and the glass transition by increasing the solution viscosity and slowing diffusion (Hunter and Weeks, 2011). Supercooling in colloidal suspensions may be important on Mars because martian soils are globally similar and contain colloidal iron-oxide dust (Morris et al., 2006; Yen et al., 2005), estimated to comprise about 3 wt.% of the soil (McSween et al., 2010).

To simplify and guide further discussion on supercooled salt solutions, we construct a ‘supplemented phase diagram’ in Fig. 7 following MacKenzie et al. (1977). A supplemented phase diagram consists of metastable states superimposed on top of an equilibrium phase diagram, with metastable regions defined by experimentally determined transition temperatures. Above the

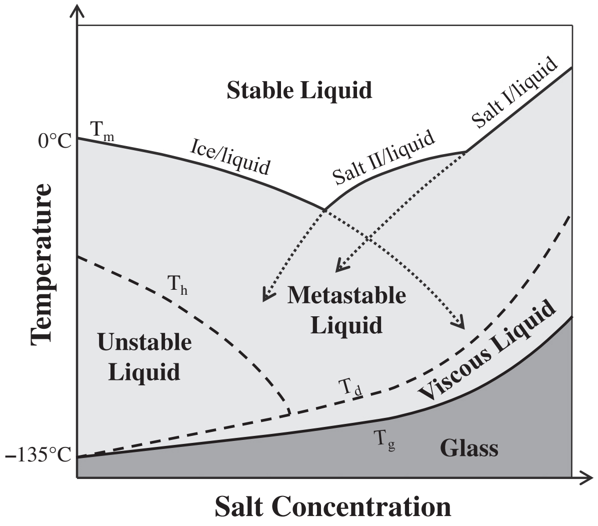

Fig. 7. A ‘supplemented phase diagram’ constructed following MacKenzie et al. (1977). Below the equilibrium melting temperature (T_m), there are a variety of metastable states that can persist over different timescales during supercooling; we categorize these states into metastable liquid, unstable liquid, viscous liquid, and glass states. The boundaries between these states, indicated by dashed lines, are defined by the homogeneous nucleation temperature (T_h), the devitrification temperature (T_d), and the glass transition temperature (T_g). Within the metastable liquid state, it is possible to have a crystalline phase in equilibrium with a metastable liquid; these are indicated by the dotted lines.

equilibrium melting temperature (T_m), an aqueous salt solution will be stable as a liquid. If such a liquid is cooled rapidly enough that crystallization does not occur, it will transition into a glass at T_g. Although the glassy state is not stable thermodynamically, it can persist for such long timescales that it can be thought of as being effectively stable. Between the stable liquid state and the effectively stable glassy state are several metastable liquid states: a viscous liquid, a metastable liquid, and an unstable liquid in order of decreasing stability. The high viscosity in the viscous liquid state greatly reduces the rate of crystal growth and nucleation. Its upper boundary is given by T_d, the devitrification temperature. The unstable liquid state is defined by the homogeneous nucleation temperature (T_h). T_h is the lowest temperature a slowly cooled solution can reach before crystallizing, and can only be approached by using very small quantities of high purity solution. Below T_h, a solution can remain liquid only for short timescales before crystallizing or transitioning to a glass. Above T_h and T_d lies the metastable liquid region, representing metastable liquid states that are typically possible to achieve with slow cooling rates. Within the metastable liquid state, as in all of the metastable states, there is a continuum of increasing relative stability. In general, the stability of metastable liquids will increase as both the temperature and concentration increase, and near the viscous state. Near T_h, metastable liquids will be highly sensitive to nucleation from kinetic effects and are not likely to occur in natural bulk fluids. Further towards the equilibrium melting temperature and at higher concentrations are the metastable liquid states that occurred in this study, which can persist in bulk solutions for at least several hours.

Of the solutions studied here, the chloride, sulfate, and the $NaClO_4$ salts all supercooled to some degree, entering into the metastable liquid state, but did not transition to a glass at the cooling rates we used. For solution concentrations that were initially slightly lower than the eutectic concentration, a similar metastable pathway was followed for all solutions; the solution supercooled until ice crystallized, after which the solution continued supercooling below the eutectic, in equilibrium with ice but metastable with respect to salt. This evolution pathway corresponds to the dotted extension of the ice/liquid line below the eutectic in Fig. 7. Finally, the solution crystallized salt to form a eutectic solid. Potentially, ice could continue crystallizing out of the metastable liquid until the glass transition was reached, resulting in a mixture of ice and glass (MacKenzie et al., 1977); however, this was not observed in this study. For solution concentrations higher than the eutectic, a greater degree of supercooling occurred (measured by ΔT_s) and a variety of metastable pathways were possible, including: precipitation of ice followed by salt, precipitation of salt followed by ice, and simultaneous precipitation of both salt and ice.

In contrast to the chloride, sulfate, and the $NaClO_4$ solutions, the $Mg(ClO_4)_2$ and $Ca(ClO_4)_2$ solutions reached the glass transition at slow cooling rates, even in soil-solution mixtures. One possible reason for the glass-forming capabilities of $Mg(ClO_4)_2$ and $Ca(ClO_4)_2$ solutions is that the eutectic temperatures of these solutions are relatively low, so that less supercooling is needed to reach the viscous or glass states. Another possible contributing factor toward the glass-forming capabilities of $Mg(ClO_4)_2$ and $Ca(ClO_4)_2$ solutions is that these salts are composed of the divalent cations Mg^{2+} and Ca^{2+}. More highly charged polyvalent ions with smaller ionic radii tend to increase electrostatic interactions in solution, which leads to greater solution viscosity (Kaminsky, 1957; Robinson and Stokes, 1965). However, the contribution of Mg^{2+} and Ca^{2+} ions to the viscosity will be counteracted by the ClO_4^- ion. Perchlorate is considered to be a powerful 'structure-breaking' ion due to its low ionic potential, which disrupts the structure of water (Walrafen, 1970) and acts to lower the solution viscosity (Kaminsky, 1957). The 'structure-breaking' ability of anions is given by the Hofmeister series in the order $SO_4^{2-} < Cl^- < NO_3^- < ClO_3^- < ClO_4^-$, for anions relevant to Mars. As a final possibility, we suggest that an ion-specific effect may occur, in which the ClO_4^- ion directly interferes with crystallization. 'Structure-breaking' ions tend to inhibit ice nucleation, as evidenced by lower homogeneous nucleation temperatures for ice (Miyata et al., 2002), and may inhibit the nucleation of salt crystals as well. This is supported by recent research into the Hofmeister series indicating that weakly hydrated 'structure-breaking' anions are strongly attracted to particle surfaces (Flores et al., 2012) and disrupt some crystallization processes (Collins, 2004; Lee et al., 2010).

Based on the previous discussion, we predict that other low eutectic temperature salts of polyvalent cations and large, 'structure breaking' anions would also easily transition into the viscous and glass states. Chlorate and nitrate ions have low ionic potentials and are predicted to occur on Mars based on atmospheric chemical modeling (Catling et al., 2010; Smith et al., 2014) and their association with each other and perchlorate in deserts on Earth (Rao et al., 2010), although they have not been detected. Ca and Mg salts of chlorate and nitrate have low eutectic temperatures; in particular, $Mg(ClO_3)_2$ is estimated to have a eutectic at −69 °C (Hanley et al., 2012), even lower than $Mg(ClO_4)_2$, and may easily transition to a glass. Another salt that is likely to be a good glass-former is ferric sulfate ($Fe_2(SO_4)_3$). The viscosity of ferric sulfate solutions is much greater than chloride salts due to the high ionic charge of both Fe^{3+} and SO_4^{2-} in solution (Chevrier et al., 2009b). Because T_g occurs when the viscosity increases to $\sim 10^{12}$ Pa s, the relatively high viscosity of ferric sulfate solutions suggests that T_g will occur at a higher temperature, even closer to the eutectic, compared to perchlorate solutions. Indeed, it is believed that the −68 °C 'eutectic' for ferric sulfate measured by Chevrier and Altheide (2008) is actually a glass transition temperature (Hennings et al., 2013a).

4.2. Implications for liquid water on Mars

The supercooling effects measured in this study indicate that salt solutions on Mars will remain liquid below their eutectic temperature for some time. In Fig. 8, the eutectic temperature of salts and their maximum supercooling measured in this study are compared with surface temperatures at the Mars Phoenix site calculated from the Mars Climate Database (MCD). For the non-glass-forming $MgSO_4$, NaCl, $MgCl_2$, and $NaClO_4$ solutions, minimum surface temperatures on Mars are always far lower than either the eutectic temperature or the supercooling measured in this study, indicating that these solutions will not remain continuously liquid over diurnal cycles. $MgSO_4$ solutions will always remain

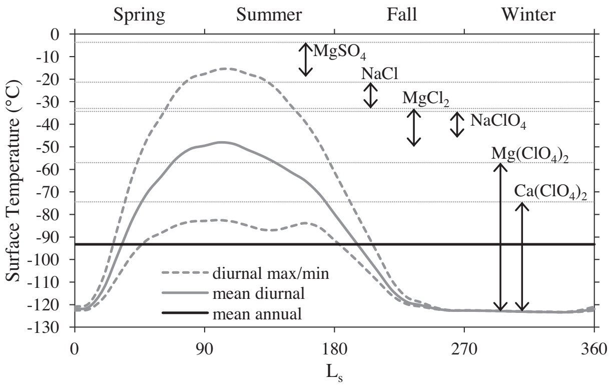

Fig. 8. Mean annual, mean diurnal, and diurnal maximum/minimum temperatures calculated using the Mars Climate Database (Lewis et al., 1999). Also shown are the eutectic temperatures of salts investigated in this study (dotted lines), with the maximum degree of supercooling found in this study indicated by arrows.

frozen because maximum temperatures never exceed the eutectic at −3.6 °C. In contrast, the eutectic temperatures of NaCl, $MgCl_2$, and $NaClO_4$ solutions are lower than warm daytime temperatures in the martian spring and summer. As a result, these salts could intermittently thaw ice to form brine during the daytime before freezing again at night.

At greater depths in the soil, the amplitude of diurnal temperature oscillations will decrease due to thermal damping. Because the thermal conductivity of dry martian soil at the Phoenix site is low, temperatures are rapidly damped to the mean diurnal temperature at a skin depth of ~5 cm (Zent et al., 2010). At even greater depths, on the order of ~1 m, the soil temperatures will approximate the mean annual temperature, which ranges from −114 °C at the poles to −69 °C at the equator (Mellon et al., 2004), and is estimated to be −93 °C at the Phoenix site based on the MCD. Mean diurnal and annual temperatures at the Phoenix site never exceed either the eutectic or the maximum supercooling measured in NaCl, $MgCl_2$, and $NaClO_4$ solutions. Hence, these solutions will be perennially frozen at depth and can only be liquid very near the soil surface at the Phoenix site. At lower latitudes than the Phoenix site, mean diurnal temperatures may exceed the eutectics of $MgCl_2$ and $NaClO_4$ solutions, allowing for the possibility of liquid solutions down to ~10 cm; however, below ~10 cm, where temperatures are damped to the annual mean, $MgCl_2$ and $NaClO_4$ solutions cannot exist as a bulk liquid because mean annual temperatures across Mars are too low.

In contrast to the non-glass-forming solutions, the glass-forming $Mg(ClO_4)_2$ and $Ca(ClO_4)_2$ solutions have the potential to stabilize liquid water on Mars over diurnal cycles, if not longer. During the martian summer, when nighttime temperatures decrease below the $Mg(ClO_4)_2$ and $Ca(ClO_4)_2$ eutectics, these salt solutions could remain in a supercooled liquid state until daytime temperatures increase above their eutectics. During the martian winter, maximum temperatures never exceed the eutectic temperatures of $Mg(ClO_4)_2$ and $Ca(ClO_4)_2$ solutions. Given that the $Mg(ClO_4)_2$ solutions we studied eventually crystallized (devitrified) during warming, $Mg(ClO_4)_2$ solutions probably undergo eutectic crystallization during the long martian winter. However, the 4 m $Ca(ClO_4)_2$ solutions never crystallized in this study, even when mixed with sediment, which suggests that $Ca(ClO_4)_2$ solutions could exist in a viscous or glassy state during the martian winter. Measured values for T_g in $Ca(ClO_4)_2$ solutions vary with concentration and range from −125 °C (2.9 m) to −112 °C (5.5 m) (Fig. 4). These glass transition temperatures are possible during the martian winter, but are close to minimum temperatures on Mars, which are limited by CO_2 condensation at −125 °C. Even if the glassy state is not common on Mars because T_g often lies close to minimum temperatures, the viscous state above T_g is well within possible temperatures on Mars.

The supercooling observed in $Mg(ClO_4)_2$ and $Ca(ClO_4)_2$ solutions suggests the possibility that liquid water may be stable on Mars for the duration of the martian spring/summer (a period of about 180 sols), and then as a viscous liquid or glass during the martian winter. Conceptually, the glassy state can be thought of as a 'liquid' because it has all of the structural characteristics of liquids, only fluid flow occurs over very long timescales due to the high viscosity (Angell, 1995). Under this consideration, concentrated perchlorate solutions may stabilize liquid water on Mars perennially, with 'liquid' water existing in states of high and low viscosity controlled by diurnal and annual temperature oscillations. To better understand the potential for such perennial 'liquids' on Mars, and possibly other icy bodies such as Europa and Enceladus, further research is needed into how long the metastable and viscous states can persist before crystallization occurs, the effect of ionic impurities on supercooling, and the potential for other salts to form glasses (e.g. chlorates, nitrates, and ferric sulfate).

4.3. The habitability of supercooled brines and potential of glasses for biological preservation

The occurrence of liquid water near the martian surface is of astrobiological interest because this suggests that present-day soils on Mars may be habitable. With respect to the $MgSO_4$, NaCl, $MgCl_2$, and $NaClO_4$ solutions studied here, even though it is possible for these solutions to be liquid during warm daytime conditions in the martian summer, the constant diurnal freeze–thaw cycle would make it difficult for life to survive. This is because eutectic crystallization is highly damaging to cell structures (Han and Bischof, 2004). $Mg(ClO_4)_2$ and $Ca(ClO_4)_2$ solutions could avoid crystallization by supercooling over diurnal cycles in the martian summer and possibly vitrifying in the martian winter. Vitrification is potentially advantageous for putative life because vitrification can preserve biological organisms, such that organisms remain viable after rewarming, and is commonly used for cryopreservation of cells (MacKenzie et al., 1977). Some organisms on Earth in cold and dry environments are known to use vitrification to enter into stasis during unfavorable conditions, thus avoiding damages from crystallization (Storey and Storey, 2004). Putative organisms on Mars could employ a similar survival strategy, using glass-forming salt solutions or organic exopolymers (Junge et al., 2006) to survive harsh conditions until more favorable conditions resumed, allowing for growth.

A central problem with the habitability of aqueous salt solutions is that high concentrations of salt will lower the activity of water, often below the limits of what is known to support growth. On Earth, the mold *Xeromyces bisporus* can grow at a water activity of 0.61, but this is an unusual case and the lower limit of water activity for growth is more commonly near 0.75 (Grant, 2004). Saturated solutions of $Mg(ClO_4)_2$ and $Ca(ClO_4)_2$ have water activities of 0.39 and 0.29 respectively at 25 °C, far lower than what life is known to tolerate. As temperatures decrease, the activity of water in a saturated solution will increase due to the removal of ions from solution by salt precipitation; however, at the eutectic temperature of $Mg(ClO_4)_2$ and $Ca(ClO_4)_2$ (using the eutectic in FREZCHEM), water activities only increase to 0.54 and 0.51 respectively, still too low for terrestrial life. A way in which water activity could increase even further is if a salt solution is warmed in equilibrium with ice. As temperatures rise above the eutectic, ice will continuously melt, diluting the salt solution and increasing the water activity; in the limit that temperatures approach 0 °C, water activity will approach one. Conversely, ice will crystallize during cooling, concentrating the remaining solution along the ice/liquid equilibrium line in Fig. 7 and extending down along the metastable line if supercooling occurs. Partial crystallization is not necessarily harmful to life because single-celled organisms can survive partial crystallization of $\geqslant$80% of the liquid water (Fahy et al., 1987). Equilibrium with ice is probable at the Phoenix site because ground-ice is present only ~5 cm below the soil surface (Smith et al., 2009). For any salt solution in equilibrium with ice, a habitable water activity of 0.6 is reached at −53.5 °C, and 0.75 at −29.6 °C. In Fig. 8, maximum daytime surface temperatures surpass −29.6 °C for a period of about 100 sols in the martian summer, and mean diurnal surface temperatures are greater than −53.5 °C for a period of about 100 sols. This suggests that liquid water with water activity suitable for growth is possible in near-surface soils at the Phoenix site for significant portions of the martian spring and summer.

Finally, we briefly consider the challenges of low relative humidity and temperature for life at the Phoenix site. Arid conditions could dehydrate salt solutions and lead to low water activities; however, the stability of near-surface ground-ice at the Phoenix site suggests that vapor transport in the soil is in equilibrium with atmospheric water vapor (Mellon et al., 2009). Given that the equilibrium vapor pressure of ice is only slightly less than pure water, salt solutions in the soil should also be stable. With respect to temperature, life on Earth has been found growing at temperatures down to about −20 °C (Junge et al., 2004; Price and Sowers, 2004; Rivkina et al., 2000), although laboratory experiments suggest that metabolism may occur at much lower temperatures (Junge et al., 2006). Recent studies have found that low ionic potential ions like perchlorate (known as 'chaotropes') will promote metabolic processes at low temperatures by disrupting ionic interactions between macromolecules, which ordinarily slow down metabolism by inhibiting protein functions at low temperatures (Chin et al., 2010; Cray et al., 2013). Hence, there is a growing body of evidence suggesting that perchlorate solutions have properties that are uniquely advantageous for low-temperature life; including, freezing-point depression, supercooling, vitrification, high oxidation potential for use in metabolic processes (Coates and Achenbach, 2004), and low-temperature stabilization of macromolecules.

5. Conclusions

Supercooled salt solutions allow liquid water to exist below eutectic temperatures, which has implications for the stability of liquid water on Mars and the habitability of present-day soils. To explore the magnitude of supercooling and its dependence of salt composition, concentration, and the presence of soil, we performed slow cooling and warming experiments on $MgSO_4$, $MgCl_2$, NaCl, $NaClO_4$, $Mg(ClO_4)_2$, and $Ca(ClO_4)_2$ solutions. The results suggest the following conclusions:

- Temperature profiles measured during these experiments indicate that $MgSO_4$, $MgCl_2$, NaCl, and $NaClO_4$ solutions supercool about 5–15 °C below their eutectic temperature and can persist in a supercooled state for several hours. Addition of soil has a variable effect on supercooling, which is surprising given that nucleation theory suggests that soil will strongly decrease supercooling due to heterogeneous nucleation on particle surfaces.
- Given the laboratory results, we suggest that during the martian summer at the Phoenix site, supercooling in $MgCl_2$, NaCl, and $NaClO_4$ solutions may increase the duration of liquid water in the daytime, but nighttime temperatures always fall below the maximum supercooling measured, indicating that these solutions will intermittently freeze and thaw. Hence, supercooled $MgCl_2$, NaCl, and $NaClO_4$ solutions will only marginally affect the stability of liquid water at the Phoenix site.
- $Mg(ClO_4)_2$ and $Ca(ClO_4)_2$ solutions supercool to a remarkable degree, down to about −120 °C, at which point they vitrify. Upon warming, some of the $Mg(ClO_4)_2$ and $Ca(ClO_4)_2$ solutions undergo devitrification, forming a eutectic mixture; however, 4 m $Ca(ClO_4)_2$ solutions, were not observed to crystallize during this study, even when mixed with soil.
- The laboratory results imply that concentrated $Mg(ClO_4)_2$ and $Ca(ClO_4)_2$ solutions could stabilize liquid water on Mars at low temperatures in viscous and glassy states over diurnal, and possibly perennial, timescales.
- The glassy state is known to be beneficial to life and protect microorganisms against damaging eutectic crystallization. Effectively, microbes can enter a state of suspended animation and be revitalized upon warming to the liquid state. Consequently, perchlorate glasses might preserve pristine cellular structures on Mars. By extension, glasses formed from brines might also be important elsewhere on other icy bodies, such as Ceres, Europa, Enceladus or Kuiper Belt Objects.

Acknowledgments

Funding from NASA Mars Data Analysis Grant #NNX10AN66G awarded to DCC. We thank Vincent Chevrier and an anonymous reviewer for their helpful comments.

References

Allen, C.C., Jager, K.M., Morris, R.V., Lindstrom, D.J., Lindstrom, M.M., Lockwood, J.P., 1998. Martian soil simulant available for scientific, educational study. Eos, Trans. Am. Geophys. Union 79, 405–409.
Altheide, T.S., Chevrier, V., Nicholson, C., Denson, J., 2009. Experimental investigation of the stability and evaporation of sulfate and chloride brines on Mars. Earth Planet. Sci. Lett. 282, 69–78.
Angell, C.A., 1995. Formation of glasses from liquids and biopolymers. Science 267, 1924–1935.
Angell, C.A., 2002. Liquid fragility and the glass transition in water and aqueous solutions. Chem. Rev. 102, 2627–2650.
Angell, C.A., Sare, E.J., 1970. Glass-forming composition regions and glass transition temperatures for aqueous electrolyte solutions. J. Chem. Phys. 53, 1058–1068.
Angell, C.A., Sichina, W., 1976. Thermodynamics of the glass transition: Empirical aspects. Ann. N.Y. Acad. Sci. 279, 53–67.
Angell, C.A., Tucker, J.C., 1980. Heat capacity changes in glass-forming aqueous solutions and the glass transition in vitreous water. J. Phys. Chem. 84, 268–272.
Bandfield, J.L., Glotch, T.D., Christensen, P.R., 2003. Spectroscopic identification of carbonate minerals in the martian dust. Science 301, 1084–1087.
Berner, R.A., 1975. The role of magnesium in the crystal growth of calcite and aragonite from sea water. Geochim. Cosmochim. Acta 39, 489–494.
Brass, G.W., 1980. Stability of brines on Mars. Icarus 41, 20–28.
Catling, D.C. et al., 2010. Atmospheric origins of perchlorate on Mars and in the Atacama. J. Geophys. Res. 115, 1–15.
Chevrier, V.F., Altheide, T.S., 2008. Low temperature aqueous ferric sulfate solutions on the surface of Mars. Geophys. Res. Lett. 35, 1–5.
Chevrier, V.F., Rivera-Valentin, E.G., 2012. Formation of recurring slope lineae by liquid brines on present-day Mars. Geophys. Res. Lett. 39, 1–5.
Chevrier, V., Hanley, J., Altheide, T.S., 2009a. Stability of perchlorate hydrates and their liquid solutions at the Phoenix landing site, Mars. Geophys. Res. Lett. 36, 1–6.
Chevrier, V.F., Ulrich, R., Altheide, T.S., 2009b. Viscosity of liquid ferric sulfate solutions and application to the formation of gullies on Mars. J. Geophys. Res.: Planets 114, 1–6.
Chin, J.P. et al., 2010. Solutes determine the temperature windows for microbial survival and growth. Proc. Natl. Acad. Sci. 107, 7835–7840.
Coates, J.D., Achenbach, L.A., 2004. Microbial perchlorate reduction: Rocket-fuelled metabolism. Nat. Rev. Microbiol. 2, 569–580.
Collins, K.D., 2004. Ions from the Hofmeister series and osmolytes: Effects on proteins in solution and in the crystallization process. Methods 34, 300–311.
Cray, J.A., Russell, J.T., Timson, D.J., Singhal, R.S., Hallsworth, J.E., 2013. A universal measure of chaotropicity and kosmotropicity. Environ. Microbiol. 15, 287–296.
Cull, S.C. et al., 2010. Concentrated perchlorate at the Mars Phoenix landing site: Evidence for thin film liquid water on Mars. Geophys. Res. Lett. 37, 1–6.
Davila, A.F. et al., 2010. Hygroscopic salts and the potential for life on Mars. Astrobiology 10, 617–628.
Dobrynina, T.A., Chernyshova, A.M., Akhapkina, N.A., Rosolovskii, V.Y., 1980. Fusion diagram of the magnesium perchlorate–water system. Russ. J. Inorg. Chem. 25, 2233–2236.
Dobrynina, T.A., Akhapkina, N.A., Rosolovskii, V.Y., 1984. The fusion diagram of the calcium perchlorate–water system. Russ. J. Inorg. Chem. 29, 1043–1045.
Ediger, M.D., Angell, C.A., Nagel, S.R., 1996. Supercooled liquids and glasses. J. Phys. Chem. 100, 13200–13212.
Ehlmann, B.L. et al., 2008. Orbital identification of carbonate-bearing rocks on Mars. Science 322, 1828–1832.
Fahy, G.M., Levy, D.I., Ali, S.E., 1987. Some emerging principles underlying the physical properties, biological actions, and utility of vitrification solutions. Cryobiology 24, 196–213.
Fairén, A.G., Davila, A.F., Gago-Duport, L., Amils, R., McKay, C.P., 2009. Stability against freezing of aqueous solutions on early Mars. Nature 459, 401–404.
Flores, S.C., Kherb, J., Cremer, P.S., 2012. Direct and reverse Hofmeister effects on interfacial water structure. J. Phys. Chem. 116, 14408–14413.
Franks, F., 1993. Solid aqueous solutions. Pure Appl. Chem. 65, 2527–2537.
Gough, R.V., Chevrier, V.F., Baustian, K.J., Wise, M.E., Tolbert, M.A., 2011. Laboratory studies of perchlorate phase transitions: Support for metastable aqueous perchlorate solutions on Mars. Earth Planet. Sci. Lett. 312, 371–377.
Grant, W.D., 2004. Life at low water activity. Philos. Trans. R. Soc. Lond.: Biol. Sci. 359, 1249–1267.
Haberle, R.M. et al., 2001. On the possibility of liquid water on present-day Mars. J. Geophys. Res. 106, 23317–23326.
Han, B., Bischof, J.C., 2004. Direct cell injury associated with eutectic crystallization during freezing. Cryobiology 48, 8–21.
Hanley, J., Chevrier, V.F., Berget, D.J., Adams, R.D., 2012. Chlorate salts and solutions on Mars. Geophys. Res. Lett. 39, 1–5.
Hecht, M.H. et al., 2009. Detection of perchlorate and the soluble chemistry of martian soil at the Phoenix lander site. Science 325, 64–67.

Hennings, E., Zürner, P., Schmidt, H., Voigt, W., 2013a. Freezing temperatures of aqueous iron(III) sulfate solutions and crystallization of a new acidic water-rich sulfate. Icarus 226, 268–271.

Hennings, E. et al., 2013b. Freezing and hydrate formation in aqueous sodium perchlorate solutions. Z. Anorg. Allg. Chem., 1–7.

Hogenboom, D.L., Kargel, J.S., Ganasan, J.P., Lee, L., 1995. Magnesium sulfate–water to 400 MPa using a novel piezometer: Densities, phase equilibria, and planetological implications. Icarus 115, 258–277.

Hunter, G.L., Weeks, E.R., 2011. The physics of the colloidal glass transition. Rep. Prog. Phys. 75, 1–56.

Ingersoll, A.P., 1970. Mars: Occurrence of liquid water. Science 168, 972–973.

Johnson, J.R. et al., 2007. Mineralogic constraints on sulfur-rich soils from Pancam spectra at Gusev crater, Mars. Geophys. Res. Lett. 34, 1–6.

Junge, K., Eicken, H., Deming, J.W., 2004. Bacterial activity at −2 to −20 °C in Arctic wintertime sea ice. Appl. Environ. Microbiol. 70, 550–557.

Junge, K., Eicken, H., Swanson, B.D., Deming, J.W., 2006. Bacterial incorporation of leucine into protein down to −20 °C with evidence for potential activity in sub-eutectic saline ice formations. Cryobiology 52, 417–429.

Kaminsky, M., 1957. Ion–solvent interaction and the viscosity of strong-electrolyte solutions. Disc. Faraday Soc., 171–179.

Kounaves, S.P. et al., 2010a. Wet chemistry experiments on the 2007 Phoenix Mars Scout lander mission: Data analysis and results. J. Geophys. Res. 115, 1–16.

Kounaves, S.P. et al., 2010b. Soluble sulfate in the martian soil at the Phoenix landing site. Geophys. Res. Lett. 37, 1–5.

Kounaves, S.P., Chaniotakis, N.A., Chevrier, V.F., Carrier, B.L., Folds, K.E., Hansen, V.M., McElhoney, K.M., O'Neil, G.D., Weber, A.W., 2014. Identification of the perchlorate parent salts at the Phoenix Mars landing site and possible implications. Icarus. http://dx.doi.org/10.1016/j.icarus.2014.01.016.

Kuz'min, R.O., Zabalueva, E.V., 1998. On salt solutions in the martian cryolithosphere. Solar Syst. Res. 32, 187–197.

Lane, M.D., Bishop, J.L., Dyar, M.D., King, P.L., Parente, M., Hyde, B.C., 2008. Mineralogy of the Paso Robles soils on Mars. Am. Miner. 95, 728–739.

Langevin, Y., Poulet, F., Bibring, J.P., Gondet, B., 2005. Sulfates in the north polar region of Mars detected by OMEGA/Mars express. Science 307, 1584–1586.

Lee, S., Sanstead, P.J., Wiener, J.M., Bebawee, R., Hilario, A.G., 2010. Effect of specific anion on templated crystal nucleation at the liquid–liquid interface. Langmuir 26, 9556–9564.

Lewis, S.R. et al., 1999. A climate database for Mars. J. Geophys. Res. 104, 24177–24194.

MacFarlane, D.R., 1986. Devitrification in glass-forming aqueous solutions. Cryobiology 23, 230–244.

MacFarlane, D.R., 1987. Physical aspects of vitrification in aqueous solutions. Cryobiology 24, 181–195.

MacKenzie, A.P., Derbyshire, W., Reid, D.S., 1977. Non-equilibrium freezing behaviour of aqueous systems. Philos. Trans. R. Soc. Lond.: Biol. Sci. 278, 167–189.

Marion, G.M., Kargel, J.S., 2008. Cold Aqueous Planetary Geochemistry with FREZCHEM: From Modeling to the Search for Life at the Limits. Springer, Berlin/Heidelberg.

Marion, G.M., Catling, D.C., Kargel, J.S., 2009. Br/Cl portioning in chloride minerals in the Burns formation on Mars. Icarus 200, 436–445.

Marion, G.M., Catling, D.C., Zahnle, K.J., Claire, M.W., 2010. Modeling aqueous perchlorate chemistries with applications to Mars. Icarus 207, 675–685.

Martínez, G.M., Renno, N.O., 2013. Water and brines on Mars: Current evidence and implications for MSL. Space Sci. Rev. 175, 29–51.

McEwen, A.S. et al., 2011. Seasonal flows on warm martian slopes. Science 333, 740–743.

McSween, H.Y., McGlynn, I.O., Rogers, A.D., 2010. Determining the modal mineralogy of martian soils. J. Geophys. Res. 115, 1–10.

Mellon, M.T., Feldman, W.C., Prettyman, T.H., 2004. The presence and stability of ground ice in the southern hemisphere of Mars. Icarus 169, 324–340.

Mellon, M.T. et al., 2009. Ground ice at the Phoenix landing site: Stability state and origin. J. Geophys. Res. 114, 1–15.

Miyata, K., Kanno, H., Niino, T., Tomizawa, K., 2002. Cationic and anionic effects on the homogeneous nucleation of ice in aqueous alkali halide solutions. Chem. Phys. Lett. 354, 51–55.

Möhlmann, D., Thomsen, K.J., 2011. Properties of cryobrines on Mars. Icarus 212, 123–130.

Morris, R.V. et al., 2006. Mössbauer mineralogy of rock, soil, and dust at Gusev crater, Mars: Spirit's journey through weakly altered olivine basalt on the plains and pervasively altered basalt in the Columbia Hills. J. Geophys. Res. 111, 1–28.

Morris, R.V. et al., 2010. Identification of carbonate-rich outcrops on Mars by the Spirit Rover. Science 329, 421–424.

Mullin, J.W., 2004. Crystallization, fourth ed. Butterworth-Heinemann, Oxford.

Mullin, J.W., Leci, C.L., 1969. Some nucleation characteristics of aqueous citric acid solutions. J. Cryst. Growth 5, 75–76.

Murchie, S.L. et al., 2009. A synthesis of martian aqueous mineralogy after 1 Mars year of observations from the Mars Reconnaissance Orbiter. J. Geophys. Res.: Planets 114, E00D06. http://dx.doi.org/10.1029/2009JE003342.

Nicholson, D.E., Felsing, W.A., 1950. The determination of the activity coefficients of the alkaline Earth and magnesium perchlorates from freezing point data. J. Am. Chem. Soc. 72, 4469–4471.

Osterloo, M.M., Anderson, F.S., Hamilton, V.E., Hynek, B.M., 2010. Geologic context of proposed chloride-bearing materials on Mars. J. Geophys. Res.: Planets 115, 1–29.

Pestova, O.N., Myund, L.A., Khripun, M.K., Prigaro, A.V., 2005. Polythermal study of the systems M $(ClO_4)_2$–H_2O ($M^{2+} = Mg^{2+}$, Ca^{2+}, Sr^{2+}, Ba^{2+}). Russ. J. Appl. Chem. 78, 409–413.

Price, P.B., Sowers, T., 2004. Temperature dependence of metabolic rates for microbial growth, maintenance, and survival. Proc. Natl. Acad. Sci. 101, 4631–4636.

Rao, B. et al., 2010. Natural chlorate in the environment: application of a new IC-ESI/MS/MS method with a $Cl^{18}O_3^-$ internal standard. Environ. Sci. Technol. 44, 8429–8434.

Reischel, M.T., Vali, G., 1975. Freezing nucleation in aqueous electrolytes. Tellus 27, 414–427.

Rennó, N.O. et al., 2009. Possible physical and thermodynamical evidence for liquid water at the Phoenix landing site. J. Geophys. Res. 114, 1–11.

Rivkina, E.M., Friedmann, E.I., McKay, C.P., Gilichinski, D.A., 2000. Metabolic activity of permafrost bacteria below the freezing point. Appl. Environ. Microbiol. 66, 3230–3233.

Robinson, R.A., Stokes, R.H., 1965. Electrolyte Solutions: The Measurement and Interpretation of Conductance, Chemical Potential and Diffusion in solutions of Simple Electrolytes, second ed. Butterworths, London.

Ruesch, O. et al., 2012. Compositional investigation of the proposed chloride-bearing materials on Mars using near-infrared orbital data from OMEGA/MEx. J. Geophys. Res. 117.

Sears, D.W.G., Chittenden, J.D., 2005. On laboratory simulation and the temperature dependence of evaporation rate of brine on Mars. Geophys. Res. Lett. 32.

Smith, M.L., Claire, M.W., Catling, D.C., Zahnle, K.J., 2014. The formation of sulfate, nitrate and perchlorate salts in the martian atmosphere. Icarus 231, 51–64.

Smith, P.H. et al., 2009. H_2O at the Phoenix landing site. Science 325, 58–61.

Spencer, R.J., Møller, N., Weare, J.H., 1990. The prediction of mineral solubilities in natural waters: A chemical equilibrium model for the Na–K–Ca–Mg–Cl–SO_4–H_2O system at temperatures below 25 °C. Geochim. Cosmochim. Acta 54, 575–590.

Stillman, D.E., Grimm, R.E., 2011. Dielectric signatures of adsorbed and salty liquid water at the Phoenix landing site, Mars. J. Geophys. Res. 116, 1–11.

Storey, J.M., Storey, K.B., 2004. Cold hardiness and freeze tolerance. In: Storey, K.B. (Ed.), Functional Metabolism: Regulation and Adaptation. John Wiley & Sons, Hoboken, NJ.

Toner, J.D., Sletten, R.S., 2013. The formation of Ca–Cl-rich groundwaters in the Dry Valleys of Antarctica: Field measurements and modeling of reactive transport. Geochim. Cosmochim. Acta 110, 84–105.

Walrafen, G.E., 1970. Raman spectral studies of the effects of perchlorate ion on water structure. J. Chem. Phys. 52, 4176–4198.

Yen, A.S. et al., 2005. An integrated view of the chemistry and mineralogy of martian soils. Nature 436, 49–54.

Zent, A.P. et al., 2010. Initial results from the thermal and electrical conductivity probe (TECP) on Phoenix. J. Geophys. Res. 115, 1–23.

Zorzano, M.P., Marti, E.M., Prieto-Ballesteros, O., Osuna, S., Renno, N., 2009. Stability of liquid saline water on present day Mars. Geophys. Res. Lett. 36, 1–4.